Institute of Condensed Matter Chemistry of Bordeaux

Growth and spectroscopic properties of ^{6}Li- and ^{10}B-enriched crystals for heat-scintillation cryogenic bolometers used in the rare events searches

R. Belhoucif, M. Velázquez, Y. Petit, O. Pérez, B. Glorieux, O. Viraphong, P. de Marcillac, N. Coron, L. Torres, E. Véron, A. Kellou, P. Veber, R. Decourt and H. El Hafid

Bulk single crystals for heat-scintillation cryogenic bolometers used in the rare events searches

- Cosmological observations have shown that baryonic matter, electrons, photons and neutrinos account for only 6 % of the total energy amount of the Universe. The existence of dark matter was assumed to explain several gravitational effects : star rotation rate distribution at the galaxy periphery, gravitational lens, missing mass for galaxy formation, etc., but never was detected directly

- Fast neutrons induced nuclear recoils can mimic the weakly interacting massive particle (WIMP) signal and constitute the ultimate radioactive backgrounds of underground experiments aiming at detecting directly particles of the dark matter halo of our galaxy. The expected neutron fluxes in underground laboratories are very weak ($\sim 10^{-6}$ n.cm^{-2}.s^{-1} for neutrons coming from natural radioactivity in the laboratory rocks and $\sim 10^{-9}$ n.cm^{-2}.s^{-1} for muon-induced neutrons), and so it is mandatory to control the growth of crystals with large masses and diameters

- Neutrinoless double beta decays in ^{100}Mo-based crystals such as $ZnMoO_4$ or Li_2MoO_4

- Very long lifetimes radioactive decays (^{209}Tl, ^{151}Eu, …)

- Solar axions to solve the “strong CP problem” of QCD, in ^{7}Li-based targets

Bulk single crystals for heat-scintillation cryogenic bolometers used in the rare events searches (2)

- EURECA experiment : 1 ton of single crystals in modules of 300 g to 1 kg

- Exploration of the WIMP's parameters space :

  - high and variable A for large spin-independent (SI) coupling and to check the A^2-dependency of the SI coupling rate ;

  - low A to enhance the sensitivity to light (~60-80 GeV/c^2) WIMPS in the cross section range $\sigma_{WIMP\text{-}nucleus} \sim 10^{-45}$-$10^{-46}$ cm^2 ;

  - non-zero nuclear spin for sensitivity to $\lambda^2 I(I+1)$-dependency (SD) interaction, $\sigma_{WIMP\text{-}nucleus}$(~10-200 GeV/$c^2$)~$10^{-42}$-$10^{-40}$ cm^2 ;

Bulk single crystals for heat-scintillation cryogenic bolometers used in the rare events searches (3)

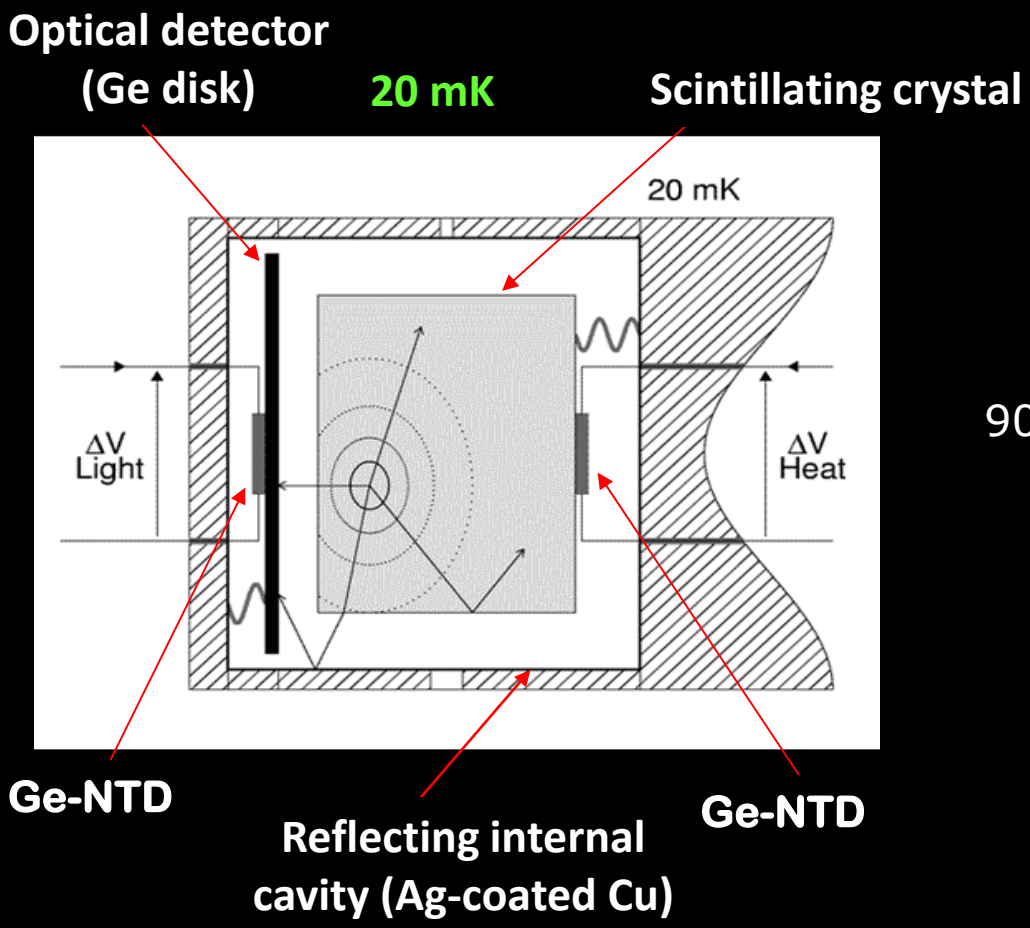

Typical collected energy conversion in LiF target :
90% heat, 3% light, 7% trapped

- As low as possible C_p(10 mK), as high as possible κ_{th}(10 mK) or θ_D(>500 K)
- No thermoluminescence, strong emitter in the 400-1700 nm spectral range
- Isotope concentrations ~10^{22} cm^{-3}, 300 g to 1 kg crystals

Relevance of $Li_6(Gd,Eu)(BO_3)_3$ crystals for neutron spectroscopy

G. F. Knoll, *Radiation detection and measurements*, 4th ed., Wiley & Sons (Ed.), 2010, chapters 14 and 15.

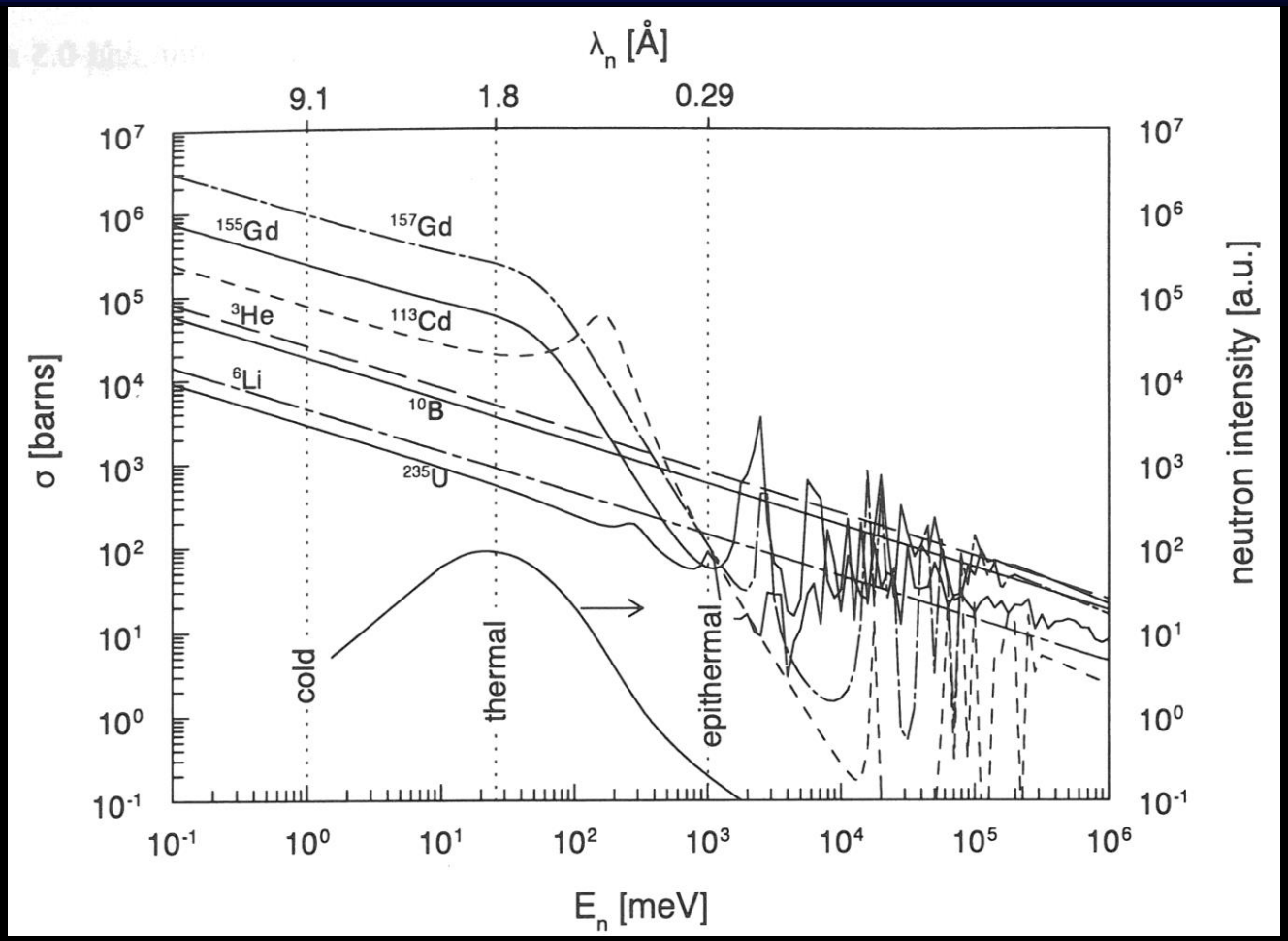

- ^{6}Li and ^{10}B isotopes, as well as several Gd isotopes, exhibit high neutron capture cross-sections ($\sigma^{10}_{B\text{-}n} \approx 4 \times \sigma^{6}_{Li\text{-}n}$(10 keV)~$8.10^{-24}$ cm^2)

- $Li_6(Gd,Eu)(BO_3)_3$ crystals constitute ideal candidates for both tailoring HSBCs with high light yields over a neutron wavelength range from 0.1 meV to 10 keV and adapting them to the cheapest light detectors available in the visible and near infrared spectral ranges

OUTLINE

- Crystal growth, chemical analysis and optical transmission properties of Li_2MoO_4 and $^{6}Li_6Eu(^{10}BO_3)_3$ crystals

- Eu^{3+} optical spectroscopy in $^{6}Li_6(Gd,Eu)(^{10}BO_3)_3$ crystals

- Selected thermodynamical properties measurements of $^{6}Li_6(Gd,Eu)(^{10}BO_3)_3$ crystals

- Conclusions

^{6}LiF, $^{6}Li_{6}(Gd,Eu)(^{10}BO_{3})_{3}$ and $Li_{2}MoO_{4}$ bulk crystal growth by combined Czochralski and Kyropoulos methods

· Low congruent melting point : 860 °C

· Platinum crucible (atm:air)/C crucible (atm:Ar)

· Growth on [4-32]-oriented LGB single crystal seed
· Growth [111]-oriented on LiF single crystal seed

· Very slow pulling and crystal rotation rates (0.2–0.4 mm/h and 7.5–10 rpm)
· Cooling: 0.3 °C/h

Thermodynamic and kinetic aspects

· High viscosity of the melt

· High supercooling (typically ~150-200 °C)

· High axial thermal gradient (~50 °C/cm)

- T ~1100°C
- Pulling rates ~1-10 $mm.h^{-1}$
- Controlled atmosphere 1 bar
- Two-zone resistive heating
- Rotation rates ~0-100 rpm
- Maximum dimensions
  ϕ~3 cm, L~5 cm

Czochralski pulling machine

- T~1500°C
- Pulling rates ~0.1-10 $mm.h^{-1}$
- Controlled atmosphere 1 bar
- Inductive heating
- Rotation rates ~0-100 rpm
- Maximum dimensions
  ϕ~3 cm, L~6 cm

^{6}LiF and $^{6}Li_6(Gd,Eu)(^{10}BO_3)_3$ crystals grown by combined Czochralski and Kyropoulos methods

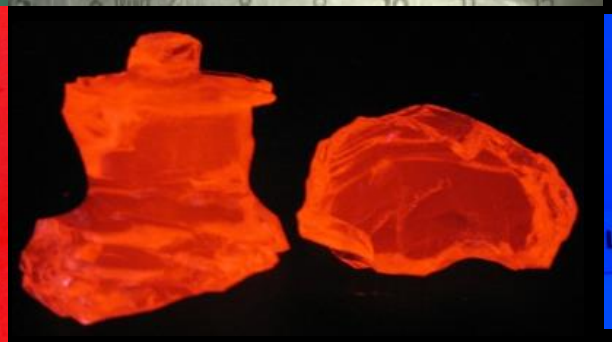

43.5 g and 17.7 g

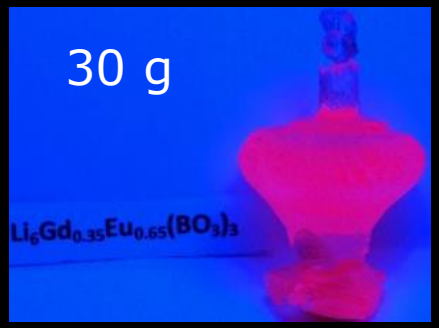

Excitation 365 nm

e=6 mm
ϕ=30 mm and 23 mm

GDMS chemical analysis of the end parts of $^{6}Li_{6}Eu(^{10}BO_{3})_{3}$ crystals

Most abundant impurities :

Gd = 7.1 10^{19} cm^{-3}, 1 atom every 73 Eu atoms
Na = 1.0 10^{19} cm^{-3}, 1 atom every 3097 Li atoms
Yb = 8.7 10^{17} cm^{-3}, 1 atom every 5978 Eu atoms
Tm = 3.8 10^{17} cm^{-3}, 1 atom every 13794 Eu atoms
Mg = 1.4 10^{17} cm^{-3}, 1 atom every 218 305 Li atoms
Lu = 1.3 10^{17} cm^{-3}, 1 atom every 39 289 Eu atoms

Minority impurities :

< 10^{17} cm^{-3} : Ca, Cu, Zn, Y, Nb, Mo, I, Tb, Hf, W, Hg
< 10^{16} cm^{-3} : Al, Si, S, V, Cr, Ni, Ga, Se, Br, Zr, Pd, Ag, Sm, Dy, Ir, Pt, Tl, Bi

Fe = 4.13 10^{15} cm^{-3}, 1 atom every 1 253 980 Eu atoms
K = less than 1 atom every 6 321 130 Li atoms
Pb = less than 1 atom every 6 699 450 Li atoms

< 10^{15} cm^{-3} : P, Cl, Sc, Ti, Mn, Co, Sr, Ge, As, Rb, Ru, In, Rh, Sn, Sb, Te, La, Ce, Pr, Nd, Ho, Er, Re, Os

Ba = 4.2 10^{14} cm^{-3}, 1 atom every 74 009 000 Li atoms

< 10^{14} cm^{-3} : Cs, less than 1 atom every 429 762 000 Li atoms
Th, U, less than 1 atom every 62 524 700/64 152 300 Eu atoms

Resulting radioactive contamination of $^{6}Li_{6}Eu(^{10}BO_{3})_{3}$ crystal

Most abundant impurities :

^{152}Gd = 0.019 mBq/kg, 1 nucleus every 36 528 Eu atoms
^{176}Lu = 16.02 mBq/kg, 1 nucleus every 1 516 950 Eu atoms

Minority impurities :

^{147}Sm < 9.55 mBq/kg, less than 1 nucleus every 5 405 670 Eu atoms
^{148}Sm < 0.008 mBq/kg, less than 1 nucleus every 7 209 170 Eu atoms
^{40}K < $3.6\ 10^{-4}$ mBq/kg, less than 1 nucleus every 54 026 800 000 Li atoms
^{87}Rb < 2.44 mBq/kg, less than 1 nucleus every 496 513 000 Li atoms
^{115}In < 0.012 mBq/kg, less than 1 nucleus every 6 465 160 Eu atoms
^{144}Nd = $1.6\ 10^{-4}$ mBq/kg, 1 nucleus every 23 329 200 Eu atoms
^{187}Re < 33.66 mBq/kg, less than 1 nucleus every 16 030 500 Eu atoms

^{232}Th < 40.72 mBq/kg, less than 1 nucleus every 62 524 700 Eu atoms
^{234}U < 0.007 mBq/kg, less than 1 nucleus every 1 188 000 000 000 Eu atoms
^{235}U < 0.041 mBq/kg, less than 1 nucleus every 8 905 090 000 Eu atoms
^{238}U < 122.56 mBq/kg, less than 1 nucleus every 6 462 130 Eu atoms

$^{6}Li_6Eu(^{10}BO_3)_3$ single crystal X-ray diffraction

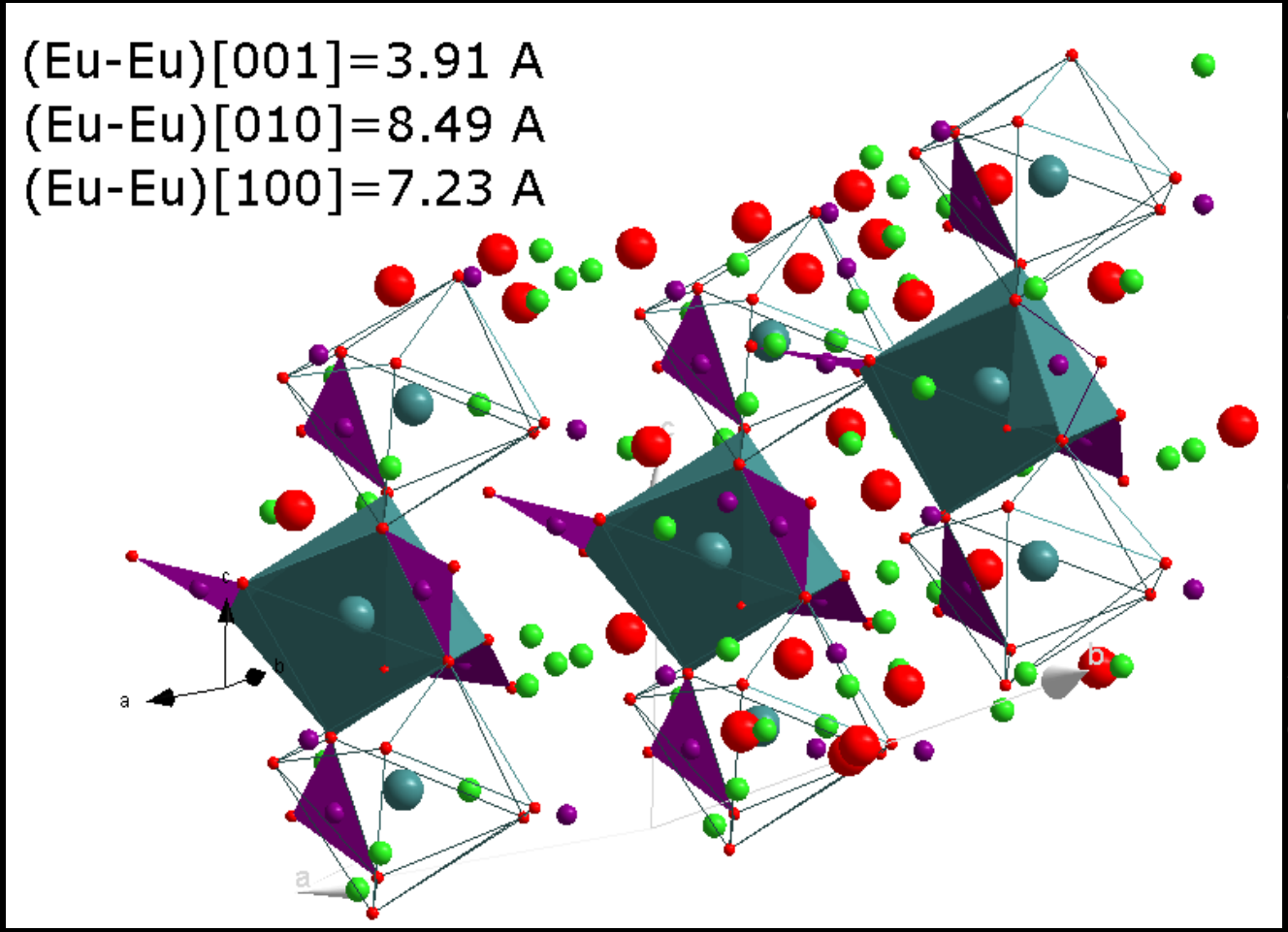

$^{6}Li_6Eu(^{10}BO_3)_3/Li_6Gd_{0.25}Eu_{0.75}(BO_3)_3$

Monoclinic P 1 $2_1/c$ 1

a=7.2318(1)Å/7.2991(2)Å

b=16.5220(3)Å/16.7478(5)Å

c=6.7033(1)Å/6.7629(2)Å

β=105.4 ^{0}/105.9 ^{0}

ρ=3.139 g.cm^{-3}/3.048 g.cm^{-3}

C_1 site symmetry

- 12 % deviation from C_s, 29 % deviation from C_2 and more than 60 % deviation from other symmetries including the inversion point ;
- $[EuO_8]$ deviation from perfect J-GBF shape ~ 25 % ;
- Connections by edges to form an infinite chain parallel to **c** lead to very low concentration quenching.

$^{6}Li_6Eu(^{10}BO_3)_3$ lattice parameters strong and anisotropic thermal expansion between RT and 948 K

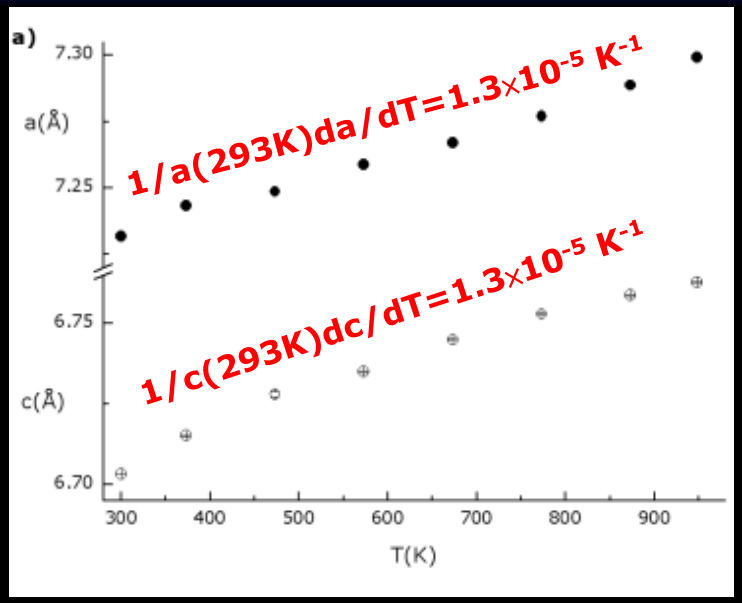

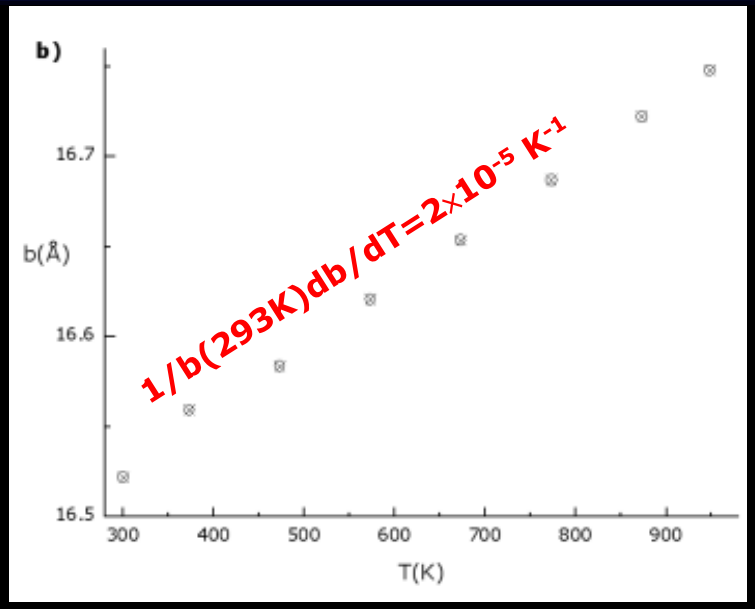

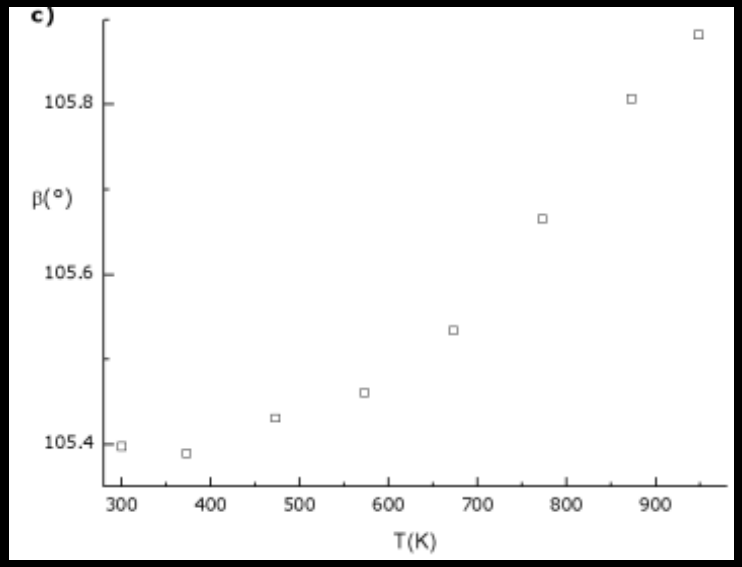

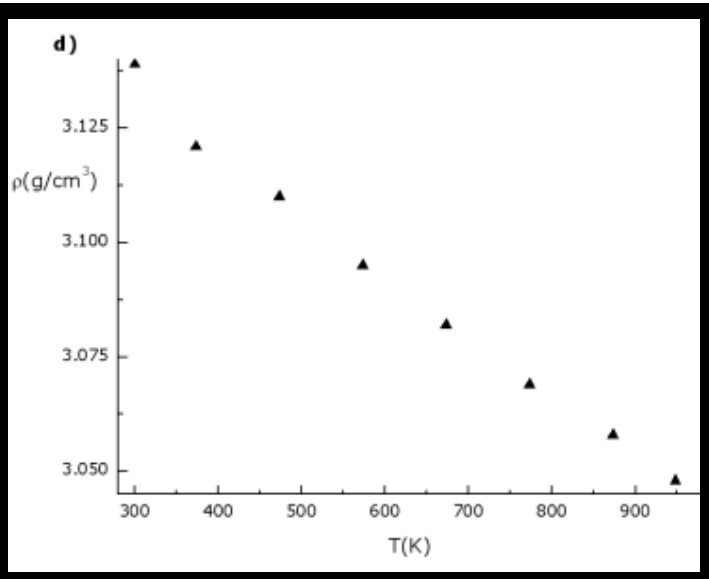

+ Minimum α-factor ~7, leading to frequent faceting (-102) & (010)

OUTLINE

- Crystal growth, chemical analysis and optical transmission properties of Li_2MoO_4 and $^{6}Li_6Eu(^{10}BO_3)_3$ crystals

- Eu^{3+} optical spectroscopy in $^{6}Li_6(Gd,Eu)(^{10}BO_3)_3$ crystals

- Selected thermodynamical properties measurements of $^{6}Li_6(Gd,Eu)(^{10}BO_3)_3$ crystals

- Conclusions

$^{6}Li_{6}(Gd,Eu)(^{10}BO_{3})_{3}$ FTIR spectra

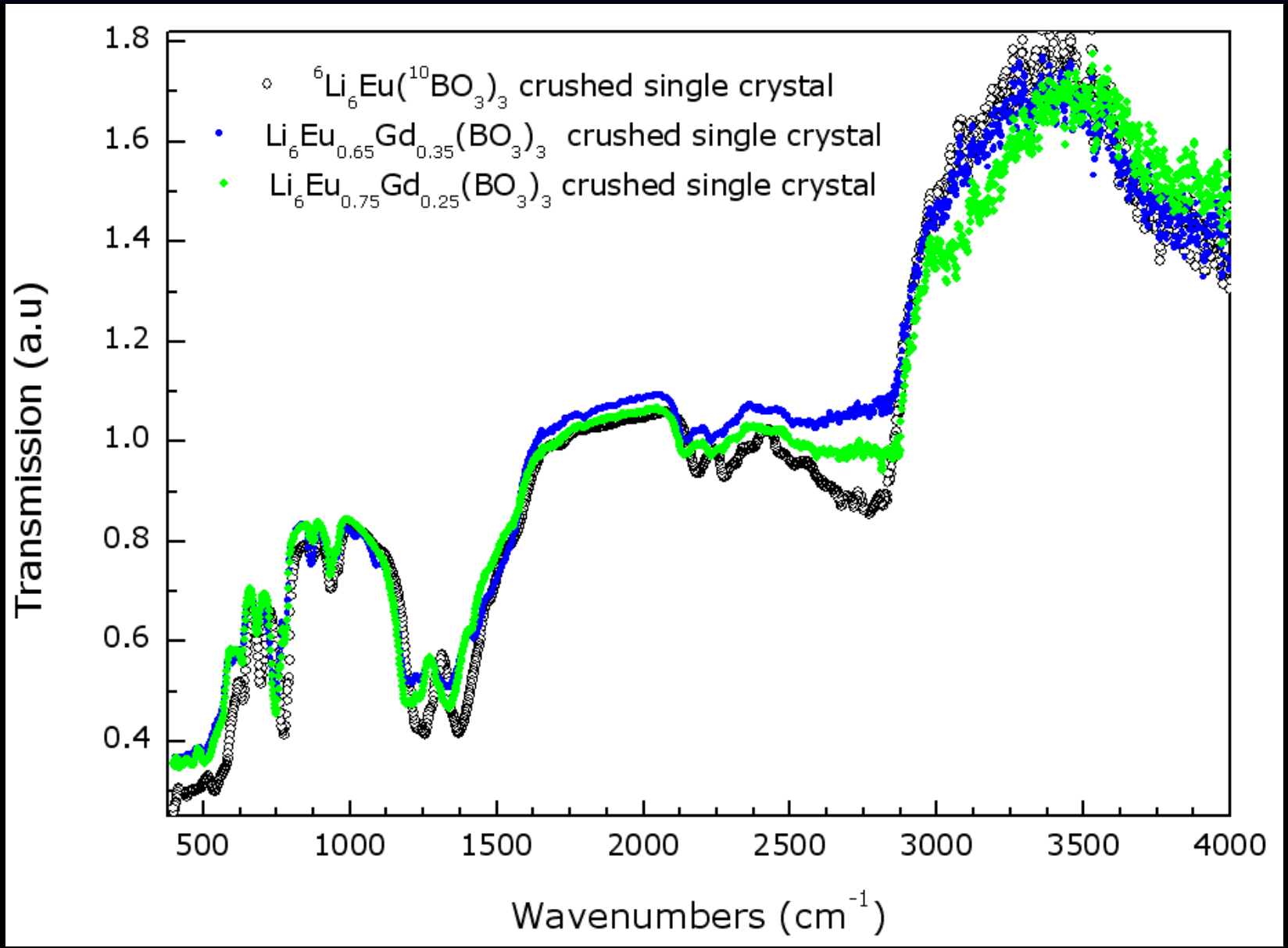

High phonon energies
No absorption due to OH^{-} groups in the 2900-3600 cm^{-1} spectral range

$^{6}Li_{6}Eu(^{10}BO_{3})_{3}$ visible and near IR polarized absorption spectra

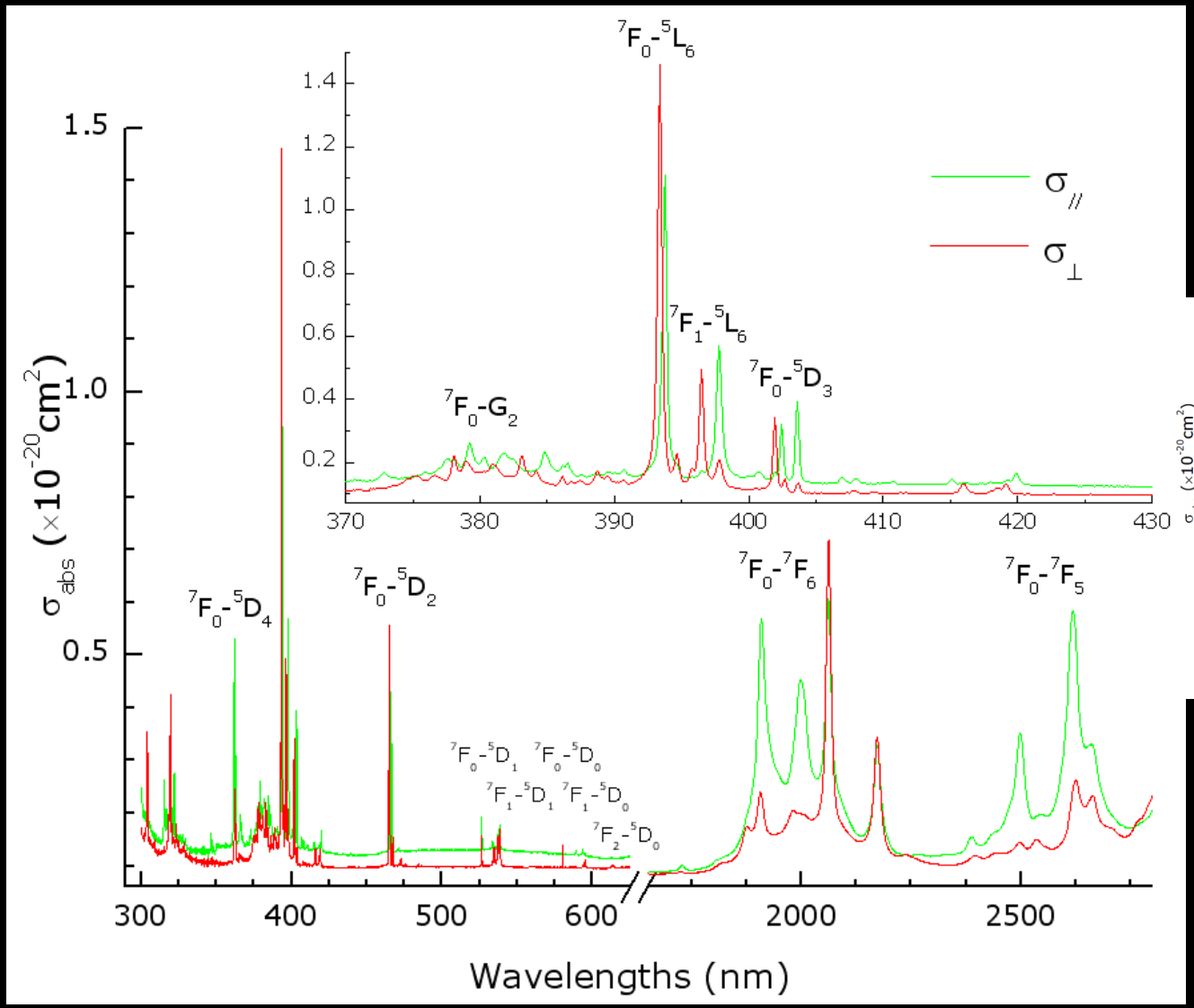

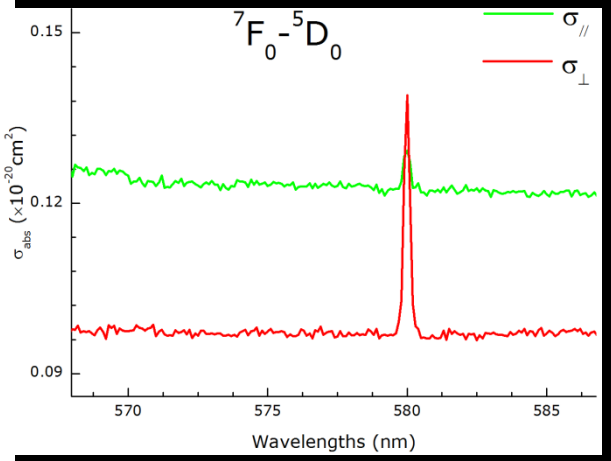

Strong and narrow absorption bands/Polarization effects/Small and single ZPL

$^{6}Li_{6}Eu(^{10}BO_{3})_{3}$ visible emission spectrum

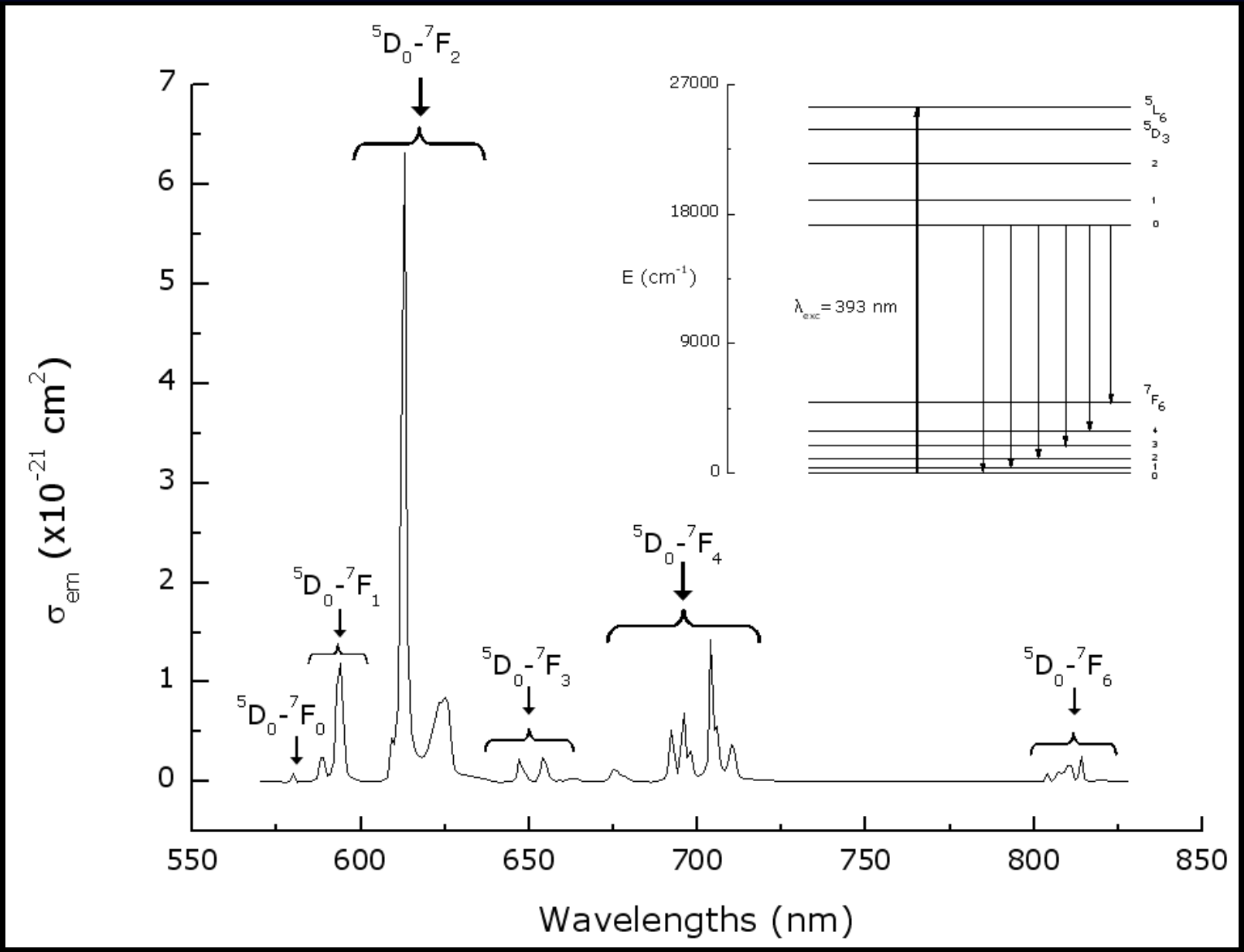

Strong, narrow and poorly polarized emission bands
Splitting of the SO multiplet degeneracy compatible with C_1 symmetry

Single crystal $^{6}Li_6(Gd,Eu)(^{10}BO_3)_3$ resonant decays at RT at 613 nm

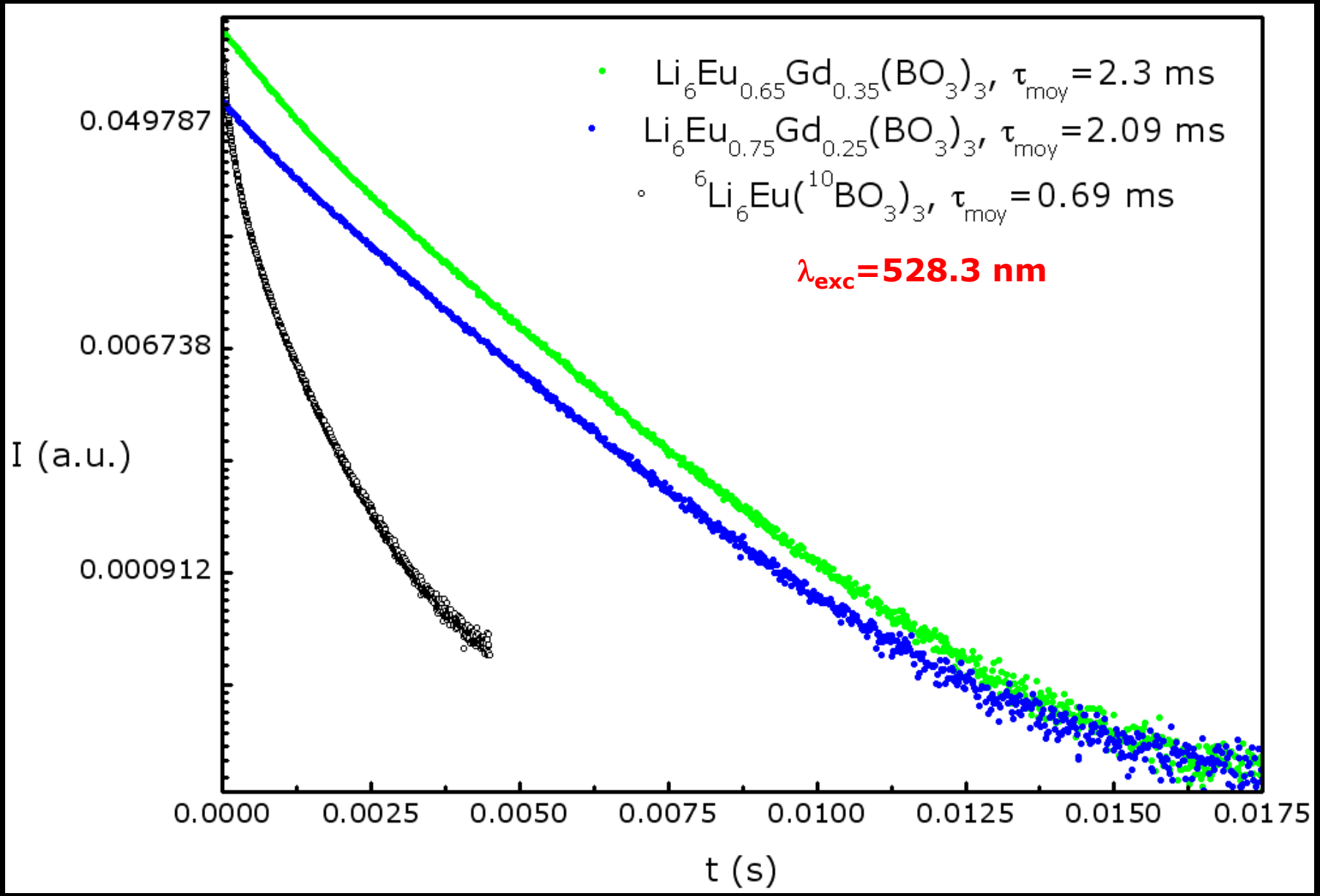

Non exponential decays for all compositions/Concentration quenching effect

Single crystal $^{6}Li_6Eu(^{10}BO_3)_3$ luminescence under X-ray excitation at RT, 77 and 4.2 K

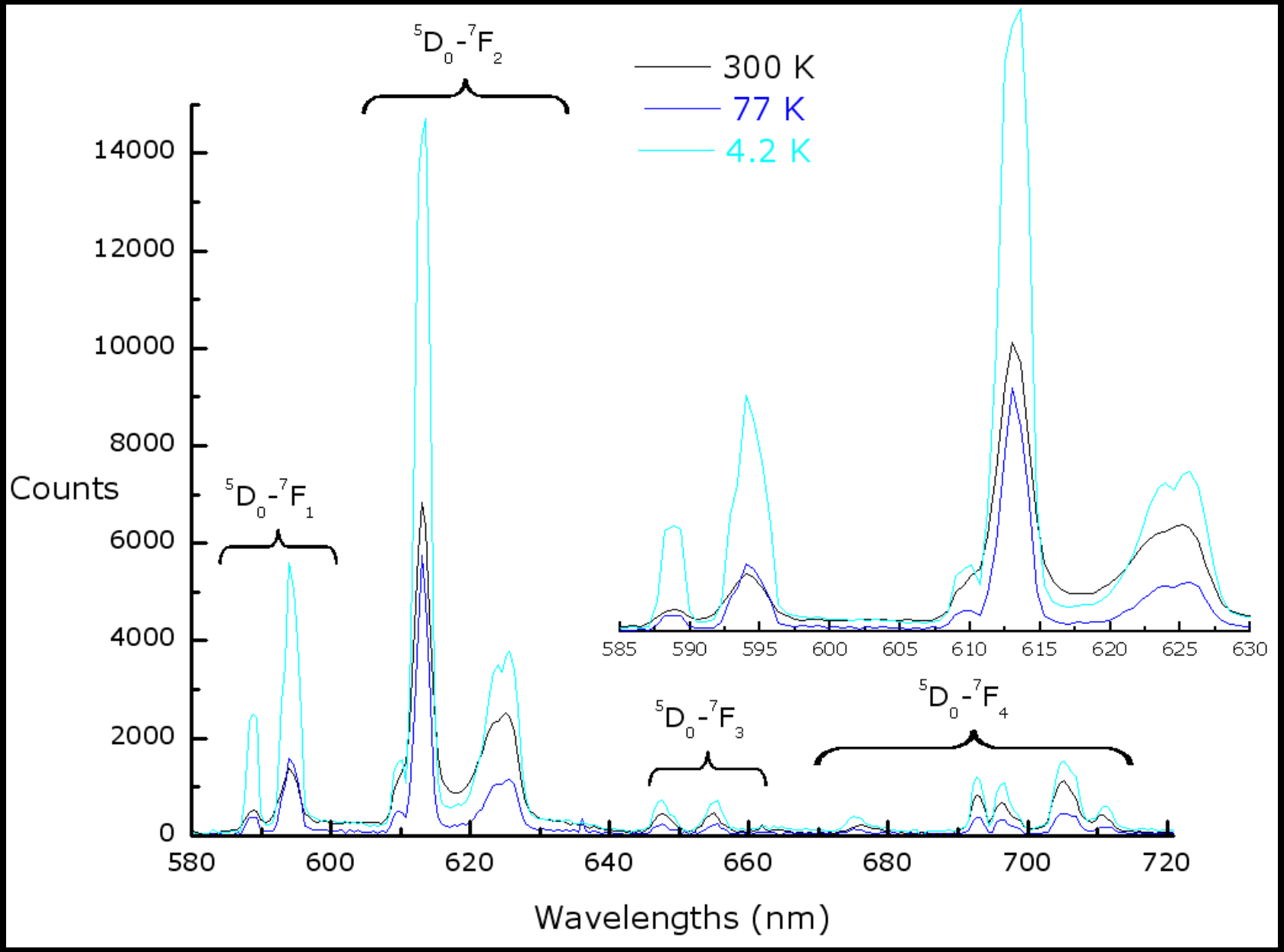

Excitation 0-40 keV, average energy 13 keV, modified by several copper and aluminum screens silver anode source (Moxtek X-ray microtube, V=40 kV, I=100 μA)

OUTLINE

- Crystal growth, chemical analysis and optical transmission properties of Li_2MoO_4 and $^{6}Li_6Eu(^{10}BO_3)_3$ crystals

- Eu^{3+} optical spectroscopy in $^{6}Li_6(Gd,Eu)(^{10}BO_3)_3$ crystals

- Selected thermodynamical properties measurements of $^{6}Li_6(Gd,Eu)(^{10}BO_3)_3$ crystals

- Conclusions

Single crystal $^{6}Li_6(Gd,Eu)(^{10}BO_3)_3$ magnetic susceptibility

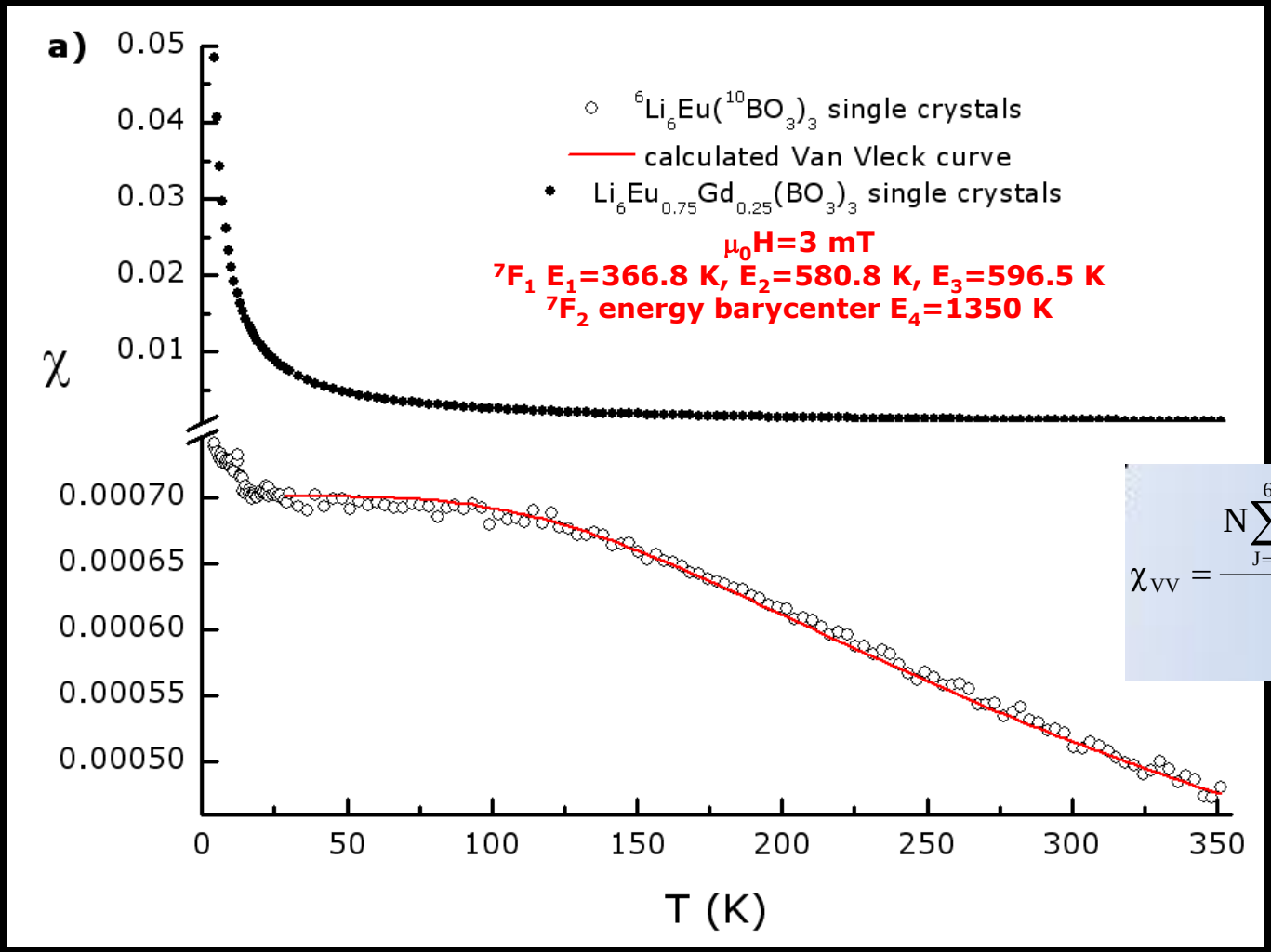

$$\chi_{VV} = \frac{N\sum_{J=0}^{6}\left[\frac{g^2\mu_B^2 J(J+1)}{3k_B T} + \alpha_J\right](2J+1)e^{\frac{-E_J}{k_B T}}}{\sum_{J=0}^{6}(2J+1)e^{\frac{-E_J}{k_B T}}}$$

- No difference between ZFC and FC measurements ;
- Typical Van Vleck paramagnetism in $^{6}Li_6Eu(^{10}BO_3)_3$, without LRO down to 4 K, checked by isothermal magnetization measurements ;
- $Li_6Eu_{0.75}Gd_{0.25}(BO_3)_3$: mixed Van Vleck and Curie-Weiss paramagnet.

Single crystal $^{6}Li_6(Gd,Eu)(^{10}BO_3)_3$ magnetic susceptibility (2)

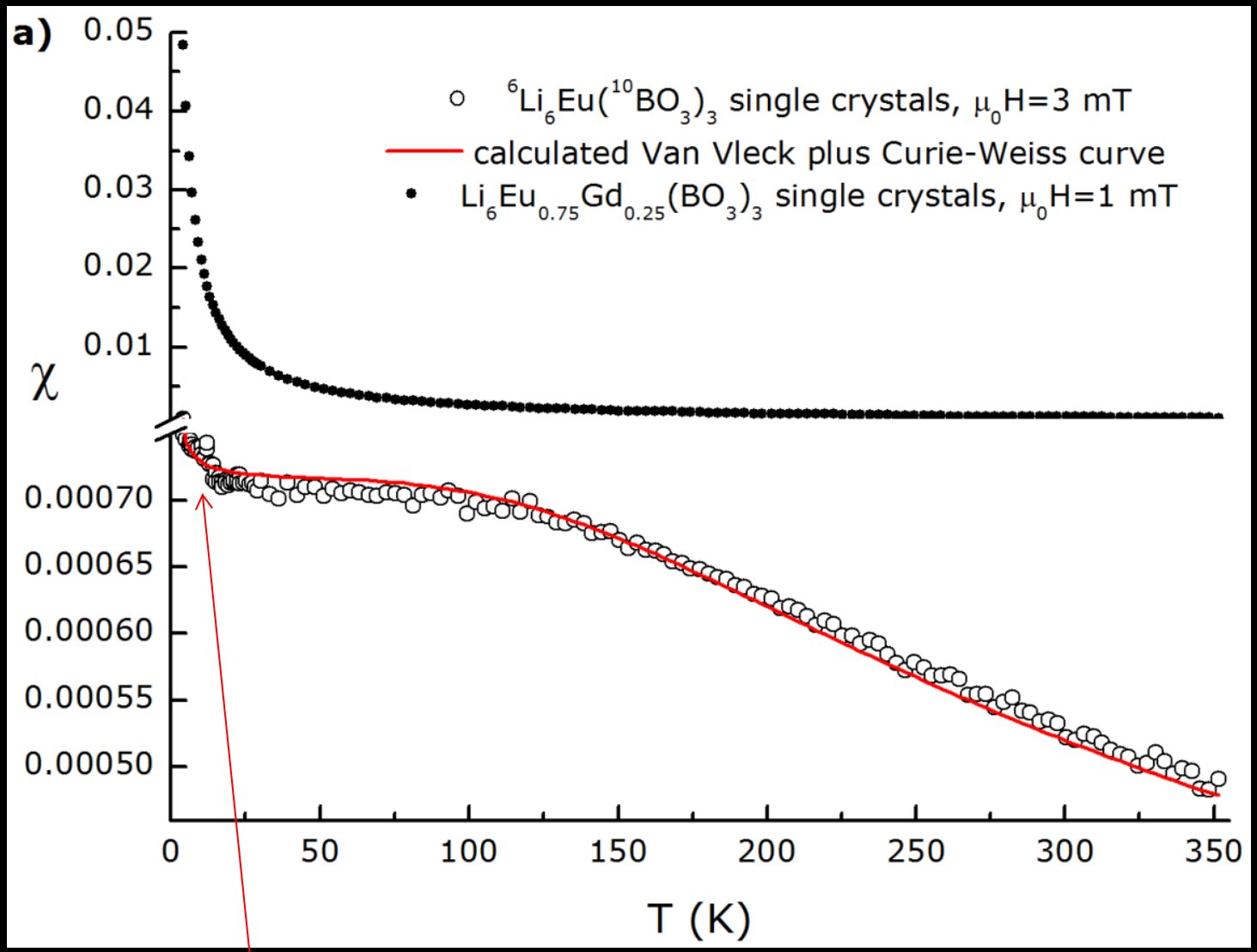

- Small rise at low temperature due to $n(Eu^{2+}/Gd^{3+})=3\ 10^{17}\ cm^{-3}$

Single crystal $^{6}Li_6(Gd,Eu)(^{10}BO_3)_3$ specific heat

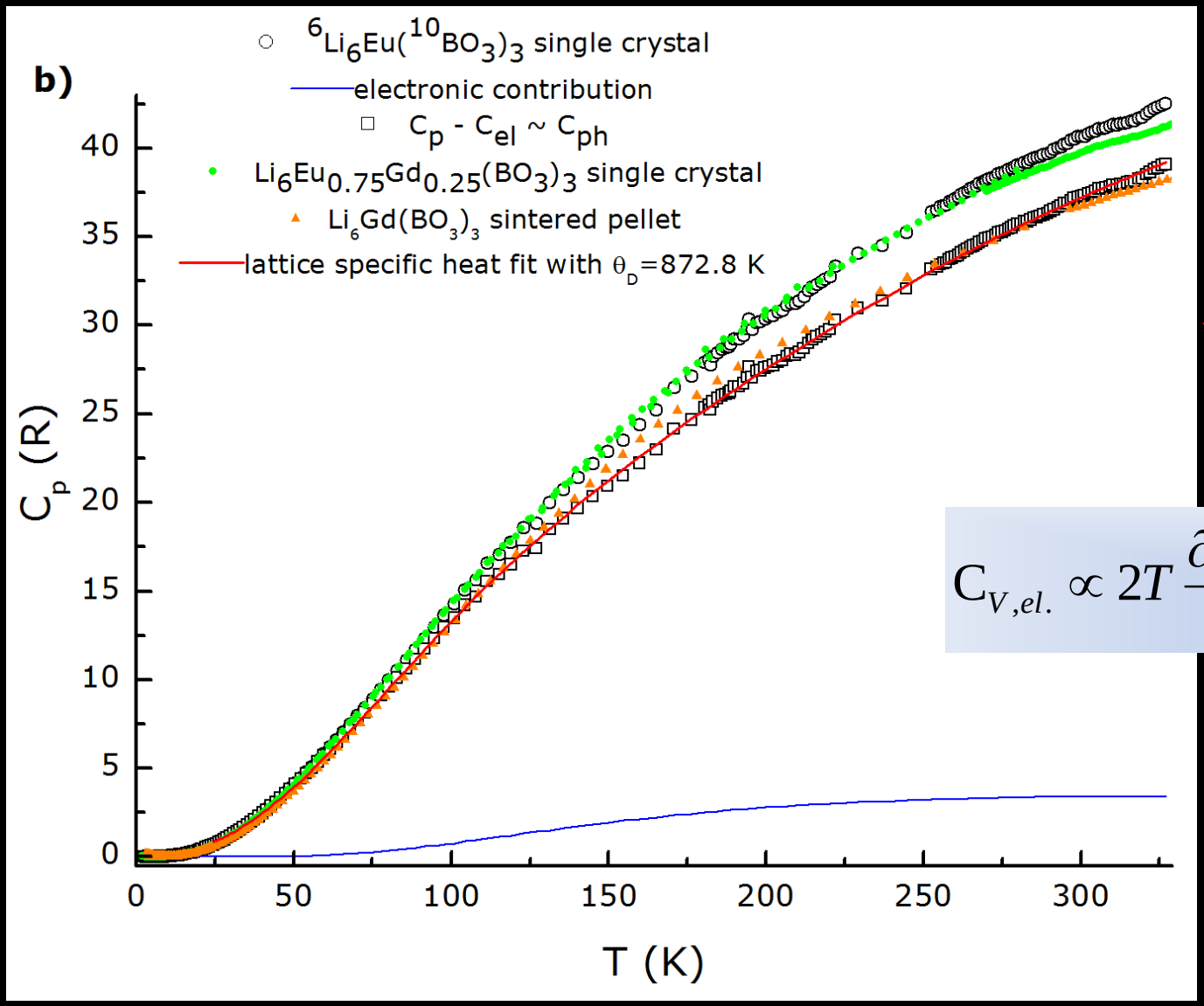

$\mu_0 H$=0 mT

$^{7}F_1$:

E_1=366.8 K

E_2=580.8 K

E_3=596.5 K

$^{7}F_2$ lowest CF sublevel :

E_4=1181.7 K

$$C_{V,el.} \propto 2T \frac{\partial \ln Z}{\partial T} + T^2 \frac{\partial^2 \ln Z}{\partial T^2}$$

- No Schottky peak nor LRO down to 2 K

$ZnMoO_4$ crystal specific heat (crystal grown at NIIC, Novosibirsk, V. Shlegel)

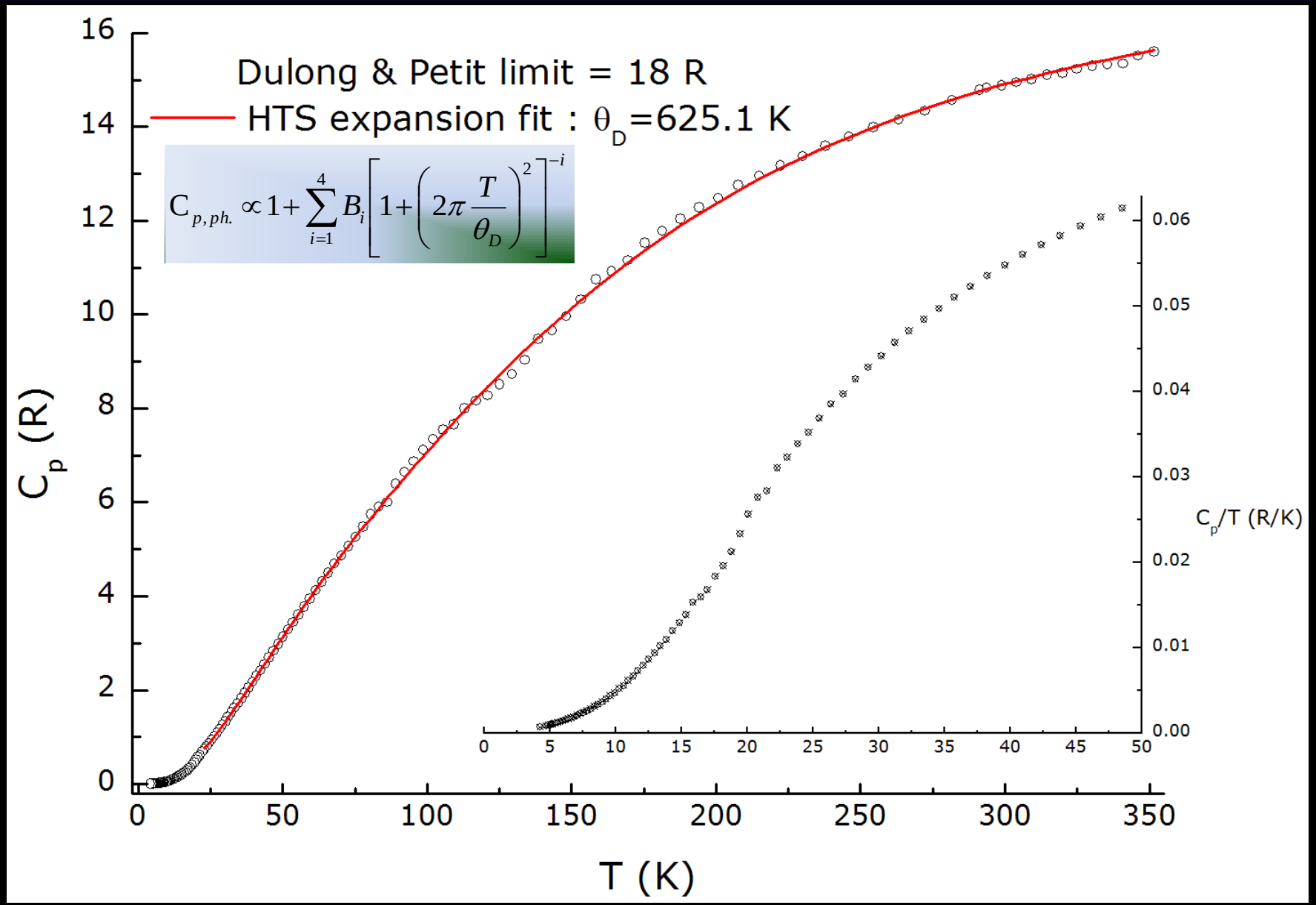

No LRO down to 4 K

$\theta_D(\alpha\text{-}Al_2O_3)$=764.8 K

Conclusions and perspectives

- We have grown new ^{6}Li- and ^{10}B-based single crystals potentially interesting for underground site neutron spectroscopy by means of HSCBs
- There remains to optimize the growth process to increase the mass, diameter and radiopurity of the crystals
- The measurements of scintillation properties, thermoluminescence and heat/light discrimination ratio across this series of compositions is in progress
- The dislocation density must be characterized and possibly analyzed

$^{6}Li_6Eu(^{10}BO_3)_3$ emission spectrum Judd-Ofelt analysis

	Ω_2 ($\times10^{-20}$ cm^2)	Ω_4 ($\times10^{-20}$ cm^2)	Ω_6 ($\times10^{-20}$ cm^2)	R	τ_R (ms)
	7.6	3.6	5.6	4.6	2.7
	σ (cm^{-1})	A_R (s^{-1})	β (%)		
$^5D_0\rightarrow{}^7F_1$	16866.4	53.8	15		
$^5D_0\rightarrow{}^7F_2$	16233.5	250.1	68		
$^5D_0\rightarrow{}^7F_3$	15324.9	-	-		
$^5D_0\rightarrow{}^7F_4$	14289.8	58.1	16		
$^5D_0\rightarrow{}^7F_6$	12334.0	5	1		
	$^{6}Li_6Eu(^{10}BO_3)_3$	$Li_6Eu_{0.75}Gd_{0.25}(BO_3)_3$	$Li_6Eu_{0.65}Gd_{0.35}(BO_3)_3$		
η (%)	25.5	~78	~85		

- Integrated intensity of the $^5D_0$-$^7F_1$ pure MD transition used as an internal reference
- R, the ratio of integrated emission intensity of the HS transition $^5D_0$-$^7F_2$ to that of the $^5D_0$-$^7F_1$ pure MD transition, suggests a low local symmetry
- Energy storage $\sigma_{em}\tau_R$ parameter (~1.6×10^{-23} cm^2.s on the $^5D_0$-$^7F_2$ transition) is quite substantial

^{6}LiF and $Li_6Eu(BO_3)_3$ crystals bolometer tests

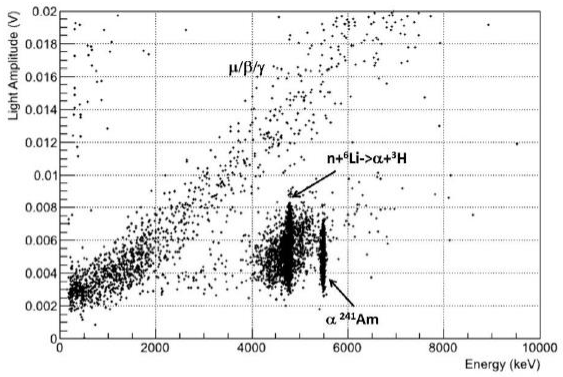

Fig. 2. Scatter plot light vs heat of a 32 g ^{6}LiF (95% enriched) exposed to a ^{252}Cf source. Thermal neutrons produce a spot at the Q_{value} of the reaction n+^{6}Li→α+^{3}H (4.78 MeV). The energy of the fast neutrons is shared between the α and ^{3}H, producing a spectrum that starts at Q_{value}. The thermal/fast neutrons band is well separated from the $\mu/\beta/\gamma$ band, but not from the α one.

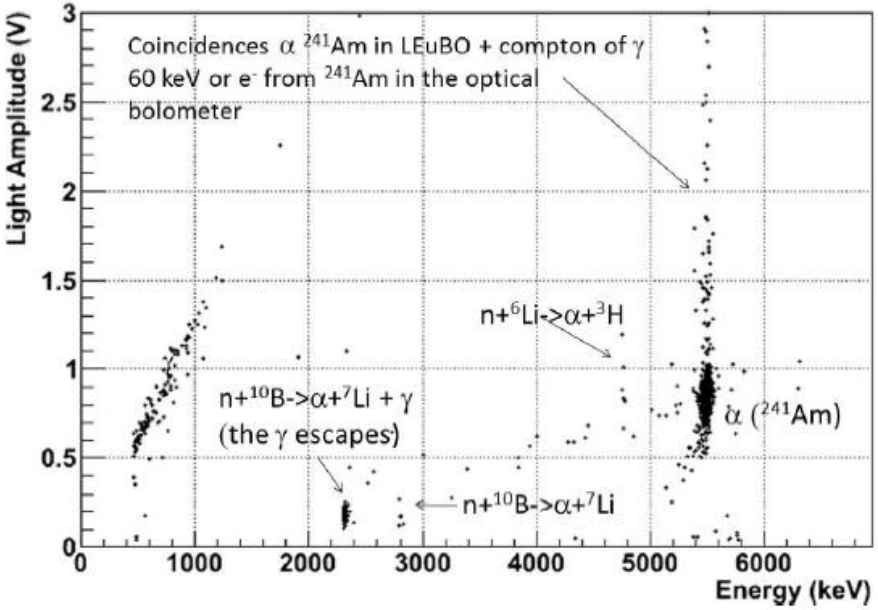

Figure 6. Same as Fig. 6 for a 5x5x5 mm^3 $Li_6Eu(BO_3)_3$ (not enriched). Also in this case the three reactions are well separated despite the poor statistics.

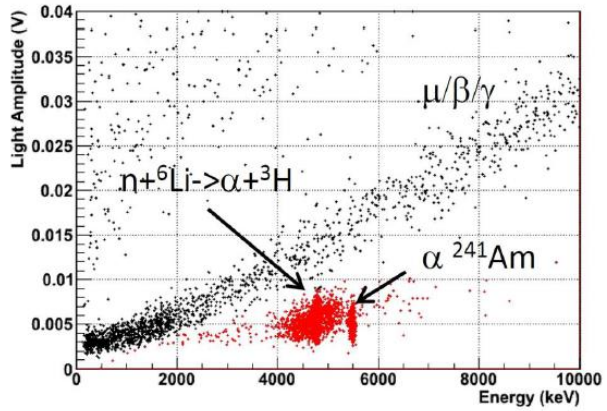

Figure 3. Scattering plot light vs heat of a 32 gr ^{6}LiF (95% enriched). The α/α+^{3}H band (in red) is well discriminated from the $\mu/\beta/\gamma$ band down to 2 MeV.

Light yield 10 times higher in LEB than in LiF
13 keV FWHM resolution in LEB versus 50 keV FWHM resolution in LiF

12th International Conference on Topics in Astroparticle and Underground Physics (TAUP 2011) IOP Publishing
Journal of Physics: Conference Series **375** (2012) 012025 doi:10.1088/1742-6596/375/1/012025